
Article:
Marvin, A.C. orcid.org/0000-0003-2590-5335, Dawson, J.F. orcid.org/0000-0003-4537-9977, Dawson, Linda et al. (3 more authors) (2004) A proposed new definition and measurement of the shielding effect of equipment enclosures. IEEE Transactions on Electromagnetic Compatibility. pp. 459-468. ISSN 0018-9375

https://doi.org/10.1109/temc.2004.831901

 DOI: 10.1109/TEMC.2004.831901

A Proposed New Definition and Measurement of the Shielding Effect of Equipment Enclosures.

Andrew C. Marvin, *Member, IEEE*, John F. Dawson, *Member, IEEE*, Simon Ward, Linda Dawson, Janet Clegg and Axel Weissenfeld

***Abstract*—This paper describes the rationale behind a new proposed measurement of the screening effect of an equipment enclosure that takes into account the contents of the enclosure. The method uses a set of representative contents for enclosures. The representative contents are equipped with surface field probes to measure the power entering the contents. The ratio of this power to the incident power density is used to derive a quantity with the dimensions of area, termed here the Shielding Aperture. The measurement technique is described and examples of measurements are given along with computed comparisons with the conventional Shielding Effectiveness of the enclosures used.**

***Index Terms*—Shielding Effectiveness Measurements, Screening Effectiveness Measurements.**

I. INTRODUCTION

The classical definition of Shielding Effectiveness (*SE*) [1,2] relates the electric field inside an enclosure E_{int} to the field that would be present at the same point in the absence of the enclosure E_0. It can be expressed as a ratio as,

$$SE = \left(E_0 / E_{\text{int}} \right) \quad (1)$$

Whilst this definition enables the comparison of the effectiveness of various enclosures to be assessed, it does not account for the presence of contents within the enclosure, the effect those contents have on the penetration of energy into the enclosure or the efficacy of the enclosure as a means to reduce the energy absorbed into its contents. The definition of shielding effectiveness is applicable for enclosures, such as screened rooms, which achieve a high level of isolation between the external environment and the internal space within the enclosure. Such enclosures have no unprotected apertures or penetrations. Enclosures used to house modern information technology equipment are not constructed to these standards and are required to achieve a lower level of shielding. They typically have apertures for ventilation and disk insertion and their contents occupy a large fraction of the internal volume of the enclosure. The energy penetration into the enclosures and the internal field distribution is, in part, determined by the enclosure contents and it may be appropriate to account for the contents in the measurement of the enclosure's shielding. In this paper we propose an alternative measure which addresses these issues and has the potential to enable equipment designers to have a measure of the interference energy that will be absorbed by the contents of a given enclosure. The definition of SE given is defined for a single position of sensing antenna. At frequencies where the enclosures are resonant this means that the results are very dependent on the frequency and the position of the antenna, making it difficult to compare the results from enclosures with different dimensions. SE can also be measured for H field at low frequencies.

Electromagnetic interference occurs in electronic equipment when an external electromagnetic wave impinges on the equipment and some of the energy conveyed by the wave is absorbed into the circuits of the equipment. The equipment shield is there to minimise this energy absorption. It is proposed here that an appropriate measure for the effectiveness of an enclosure should be based on the energy absorbed by a set of representative enclosure contents when the enclosure and its contents are illuminated by an incident electromagnetic wave of defined power density or field strength. It is possible that for some circuit types the energy absorption is not the most appropriate measure as for some device technologies (eg MOS transistors) high impulse transients can cause flashover effects and damage the circuits. However, it is likely that an enclosure containing circuits which absorb energy is less likely to resonate such that a high field strength is generated inside the enclosure. Therefore the measure proposed gives a more appropriate measure than the SE which can significantly over or underestimate the field which might be generated inside the enclosure due to an external threat.

Current standards [1 (withdrawn) and 2] are defined for

This work was funded by the Engineering and Physical Sciences Research Council.

Andrew Marvin, John Dawson, Janet Clegg and Linda Dawson are with the Department of Electronics at the University of York, England (phone: +44 1904 432342 , email: acm@ohm.york.ac.uk).

Simon Ward is with Accent Optical Technologies, York, UK

Axel Weissenfeld is a student with University of Hannover,

larger enclosures (i.e. greater than 2m dimensions) but are not appropriate for smaller enclosures such as those which house most IT electronics. Although [2] is being revised and a section on techniques for smaller enclosures is expected the techniques to be defined are still under discussion, possibilities include stirred mode and conducted techniques (e.g. current injection, transfer impedance)[3,4,5]. The techniques presented here are more appropriate to smaller enclosures and have the advantage over some of the other techniques that the results would be appropriate to loaded enclosures and could reduce the possibility of using over specified enclosures. Other methods have been proposed and used for the measurement of screening effectiveness of screening cans for mounting on circuit boards [6].

The work presented here is the result of a preliminary computational and experimental study of the concept. The technique has been demonstrated and results are presented. It should be recognised however that further detailed development is required before the technique can be used. In particular, a set of standardized representative enclosure contents needs to be defined.

II. Shielding Aperture and Energy Absorption in Electronic Systems

Consider an enclosure with contents that absorb some of the incident power on the enclosure through enclosure imperfections. The incident power density is P_I W/m^2 and the absorbed power is P_A W. An enclosure acting as an efficient shield would minimise the value of the ratio of P_A to P_I, a quantity with dimensions m^2. We define this quantity, the Shielding Aperture (*SA*) of the enclosure, as

$$SA = \left(P_A / P_I \right) \tag{2}$$

The SA defined above is a function of the direction of arrival and the polarization of the incident wave on the enclosure, as is the SE for the same enclosure.

The SA of an enclosure depends as much on the exact nature of the contents as it does on the enclosure itself. For this reason, if the SA is to be used as a measure of the shielding of an enclosure, the contents must be standardised. In practice, no electronic circuits comprising the contents of an enclosure are 'standard', however a set of representative contents (RC) can be defined that has the energy absorbing properties of typical electronic systems. In [7] it was shown that for computational modeling purposes, a populated circuit card can be represented as a homogeneous sheet of resistive material defined by its sheet resistivity or by reflection and transmission coefficients, depending on the requirements of the computational algorithm. This has been extended in this work to the use of a thin carbon loaded foam block as the RC replicating the circuit card. Such a block is shown in Fig. 1. The use of a thin foam block is considered to be representative of a circuit board in that the effect of the thin block on the Q of resonances is similar to that of a populated circuit card of the same area. The advantage of using a foam block instead of a thin resistive sheet is that the block's thickness can be adjusted to obtain the best results from a limited set of foams with differing electrical properties. The foam used in this work is not commercially available but was a sample set provided for research purposes, and the set has properties similar to those used in multilayer absorbers.

The advantage of a homogeneous load is that the power absorbed can be estimated from a knowledge of the electrical parameters of the material and the surface currents. The surface current can be measured by measuring the surface magnetic field using magnetic field sensing loops placed as shown in Fig. 1.

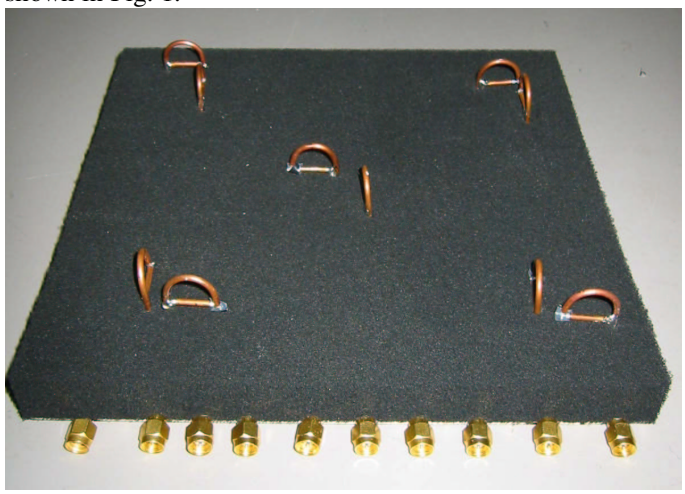

Fig. 1. A Representative Contents showing the carbon loaded foam block with magnetic field sensing loops and a ground-plane.

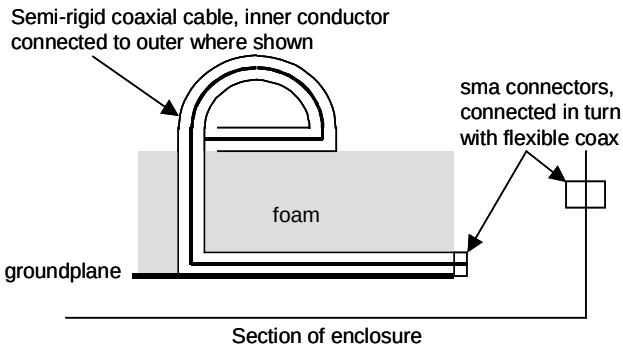

Fig.2 Showing construction method the loops and RC (internal dimensions of loop are 9 mm high by 14 mm wide)

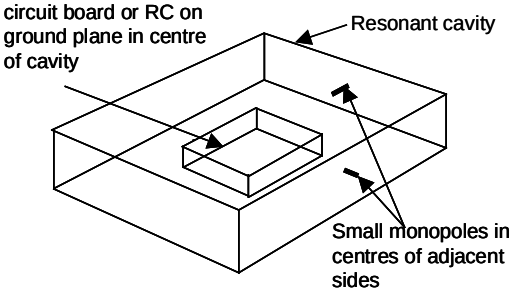

Fig.3 Showing position of small monopoles and circuit board/RC in resonant cavity for test purposes

The RC has a ground-plane on the bottom as shown in Fig.2, with the carbon-loaded foam on one side representing the device population. The block illustrated in Fig. 1 has dimensions 200 mm by 200 mm by 20 mm, equal to the area of the card chosen to provide a 'reasonable' fill of the enclosure tested. The loops and connectors allow the measurement of the tangential surface magnetic field at a number of positions on the RC. The loops are electrically small in the frequency range used.

The properties of the RC material (thickness and foam type from available set) are chosen by comparison with a populated circuit card of the same area. This is an experimental process and results in a RC with electromagnetic properties representative of a particular population density and device technology. Each circuit board or block of foam is placed at the same position in a resonant cavity of comparable size to an enclosure. The cavity is probed by two short monopoles (see Fig.3) and the forward scattering parameter S_{21} between the two monopoles is measured. The properties of the RC, foam thickness and type are selected for best match of resonant frequencies and Q factors. A typical result is shown in Fig.4 where a PC controller card of dimensions 240 mm by 90 mm was placed in a 400 mm by 400 mm by 125 mm enclosure. The material used in the measurement of Fig.4 was chosen to make the RC shown in Fig. 1. Clearly the match between the PCB and the RC is not perfect and the match is better at lower frequencies. The results presented here are representative of the match that can be obtained with this form of RC. Individual RCs can be made for different sizes of circuit card and various device technologies. RCs with carbon-loaded foam on both sides have also been used. Based on a least-means squares fit using the reflection coefficient of a 10 cm thick sample measured in a coaxial jig in the frequency range 30 MHz to 1.3 GHz, the material parameters were found to be approximately ε_r=1.27 and σ=0.03 S/m.

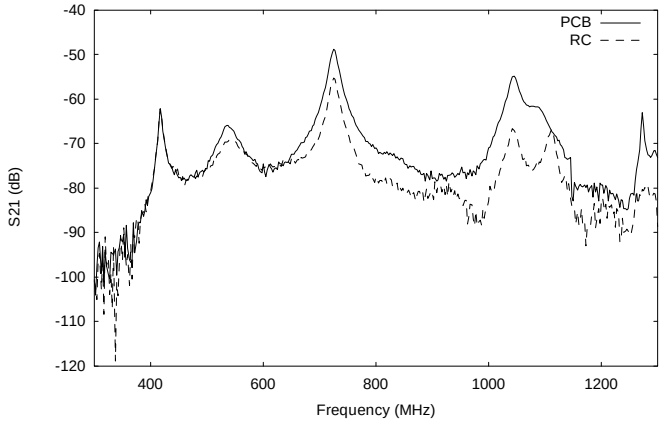

Fig. 4. Comparison of the frequency response of a cavity loaded with a PC controller card (PCB) and an RC of the same size (RC).

III. Comparison of SA Computations from Poynting Vector and Magnetic Field Predictions Using TLM

Energy penetrating an enclosure through its apertures is absorbed into the enclosure contents. In order to enable the measurement of the absorbed energy it is necessary to evaluate the distribution of energy flow around the RC inside the enclosure. This can only be done computationally. The TLM algorithm was used for this purpose.

Fig. 5 shows three computed graphs of SA for the same enclosure RC combination, a 400 mm by 400 mm by 120 mm enclosure with the RC shown in Fig. 1 mounted centrally in the enclosure volume. The enclosure is modeled with a 190 mm by 60 mm aperture in one face. The 'Poynting' graph is derived by integrating the computed Poynting vector over the surface of the RC accounting for both positive (ingoing) and negative (emergent) power flow. Note that the units of SA are expressed logarithmically as dBm^2 in this and subsequent figures.

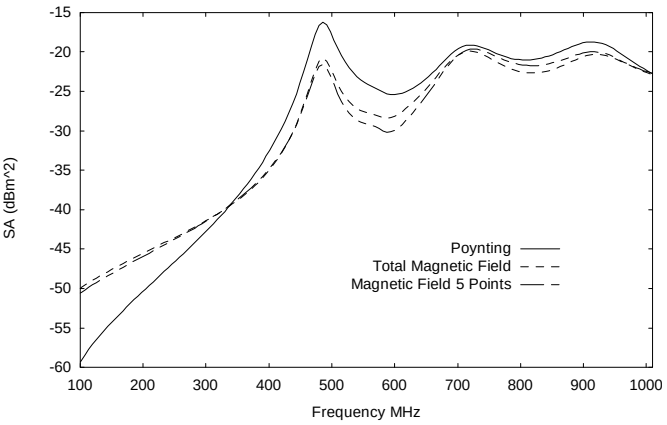

Fig. 5. Comparison of the results of 3 methods of computation of SA

The curve marked 'Total Magnetic Field' is computed by using the tangential magnetic field values at the RC surface and the modified surface resistance (R_{sm}) values computed as described below in section IV B. In this case the direction of energy flow is not discriminated and it can be seen that emergent energy, which is found to be mostly at the RC edges, has little effect on the computation of total power absorbed at frequencies in excess of 200 MHz, the maximum error of 5 dB being at the damped resonance frequency at 470 MHz. Emergent energy from the edges of the RC is more significant at lower frequencies where the carbon loaded foam block of the RC is electrically very thin. The third curve is computed using magnetic field values at five sample positions on the RC surface with linear scaling of the measured power according to the area ratio. The five points are in the centre of one face and the four corners of the same face (as shown on the RC of Fig. 1). The similarity of the results is such that it is possible to obtain an adequate estimate of the SA by a limited set of measurements of the power flow on the RC. Similar computations for other RC geometries and enclosures

verify the generality of this result. The loop spacing is set by the probability of loops coinciding with more than one field minimum in the damped resonant enclosure and hence the probability of a significant difference between the total power absorbed and the estimation from the measurements. The number of points sampled is thus set by the loop spacing and it is suggested that the upper limit of frequency should be set such that the spacing between sensors is less than one half wavelength. This is demonstrated for a larger enclosure in section V.

A. *Positioning of the RC*

Results of measurements and modeling indicate that the position of the RC within the enclosure is not critical providing the RC is not placed directly in front of a large aperture. Above the first resonance it was found that moving the RC around the enclosure (including varying the height) made less than 3 dB difference over most of the frequency range up to 2 GHz. Below the first resonance the proximity of the RC to the aperture can have significant effect (depending on the dimensions of the enclosure).

With the loops positioned on the RC as shown in Fig. 1, the proximity of the RC to the nearest conducting wall was not found to have a significant effect in either measurement or computation

IV. Theory of the Measurement of Shielding Aperture

Equation 2 gives the SA as the ratio between the power density incident at a point and the power absorbed by an enclosure contents. If we consider the representative contents (RC) the power density entering the RC is related to the local surface magnetic field at loop n (H_{sn}) and the real part of its modified surface resistance (R_{sm}), see section IV B. The total power entering the RC P_A is estimated by;

$$P_A = \frac{A}{N}\sum_{n=1}^{N}\left|H_{sn}\right|^2 R_{Sm} \tag{3}$$

where the total absorbing surface area A of the RC and the surface area is sampled by each of N loops each given equal weighting.

A. *Measurement system and calculation*

The measurement system comprises a transmitting antenna with gain G in an anechoic chamber illuminating the enclosure containing the RC. The separation between the antenna and the enclosure r is typically 3 m as in a standard EMC immunity measurement. The power density incident on the enclosure is P_I,

$$P_I = {P_T G}\Big/{4\pi r^2} \tag{4}$$

where P_T is the power input to the transmitting antenna. The SA is,

$$SA = \frac{4\pi r^2 A}{P_T G N}\sum_{n=1}^{N}\left|H_{sn}\right|^2 R_{sm} \tag{5}$$

The measurement instrumentation comprises a network analyzer. A set of measurements of the forward scattering parameters for each of the N loops S_{21n} is made with port 1 driving the source antenna and port 2 connected to each of the loops in turn. The surface magnetic fields are measured using the individual loop's calibration (K_n) which is measured with a known field in an anechoic chamber. The voltage at the input of the network analyzer from loop n is V_n, such that,

$$H_{sn} = K_n V_n \tag{6}$$

Assuming the network analyzer operates with reference impedance Z_0, the S_{21} for loop n is defined by (7),

$$\left|S_{21n}\right|^2 = \left({\left|V_n\right|^2}\Big/{Z_0 P_T}\right) \tag{7}$$

The SA is thus,

$$SA = \left({4\pi r^2 Z_0 A R_{sm}}\Big/{GN}\right)\sum_{n=1}^{N}\left|S_{21n}\right|^2\left|K_n\right|^2 \tag{8}$$

This formulation of SA is simplified for clarity. In practice, cable losses and transmitting antenna mismatch losses are included as is the gain of any transmitting power amplifier or receiving pre-amplifier. It should be noted that the practical measurement of SA does not require a measurement of the incident power density as long as the parameters of equation 8 are known. The measurement technique relates the ratio of the incident power density to the absorbed power through the forward scattering parameter.

B. *Calculation of Modified Surface Resistance*

Whilst it would appear that the surface impedance of the layer could be calculated analytically, using an infinite sheet approximation and knowledge of the material parameters, the edge effect due to the finite size of the representative contents was found to be an important factor in determining the energy absorbed. Thus a modified surface resistance parameter is required in this application. It can be seen in Fig. 6 that the SA of a finite sheet is much larger than would be expected by considering the energy absorbed by the same area forming part of an infinite sheet either by using an analytical model or by a TLM simulation. This effect is particularly apparent at low frequencies.

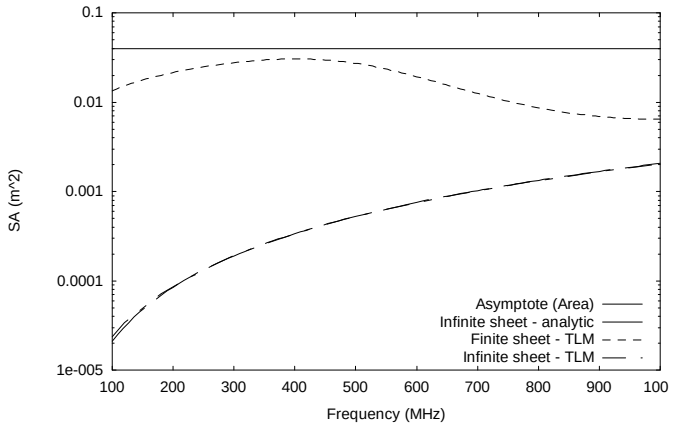

Fig. 6: Comparing the Infinite sheet, free-space, analytical approximation for SA calculation for normal incidence (model) with TLM models of infinite and finite sheets. The actual area of the 200 x 200 x 20 mm representative contents is also shown.

Therefore the frequency dependent modified surface resistance (real part of surface impedance) data was estimated numerically using a Transmission Line Matrix (TLM) model to determine the ratio of energy absorbed to the square of the surface tangential magnetic field (H_T^2). The constitutive parameters of the foam, for use in the TLM model, were determined using reflectivity measurements of a 10cm thick sample in a coaxial test-jig. The real part of the surface impedance, $\Re[Z_S]$, is determined by taking the ratio of mean power absorbed over the surface to the mean-squared value of the tangential magnetic field and has been termed 'modified surface resistance':

$$R_{Sm} = \Re[Z_S] = \frac{\langle \Re[S_N] \rangle_S}{\langle H_T^2 \rangle_S} \qquad (9)$$

where S_N is the Poynting vector of the incident wave (normal to the surface), and H_T is the magnitude of the tangential component of the magnetic field at the surface of the absorber and $\langle\ \rangle_S$ indicates an average over the absorbing surface. The modified surface resistance values calculated for the RC of Fig. 1 and used in subsequent measurements are shown in Fig. 7. The increasing value with frequency is to be expected as the effect of the RC ground-plane on energy incident on the top surface diminishes.

V. Comparison of Modeled Results and Measurements of Shielding Aperture.

The SA results for enclosures with a RC are presented below for enclosures of 300 mm square and 480 mm square representative of small enclosures up to 19 inch rack size (480 mm). Each enclosure was measured with apertures of appropriate size. The real effect of the enclosure can be judged by measuring the power absorbed in the RC without an enclosure and comparing it to the incident power density to give an effective SA value. Fig. 8 shows this effective SA value for the RC of Fig 1 measured in the anechoic chamber along with the TLM simulation of the same quantity.

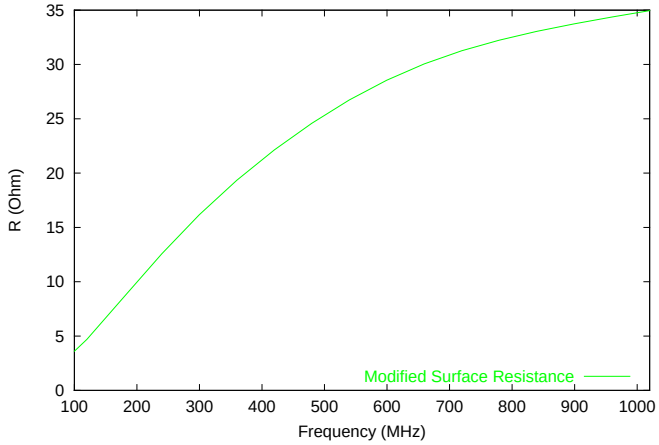

Fig. 7. Calculated values of Modified Surface Resistance for the RC of Fig. 1.

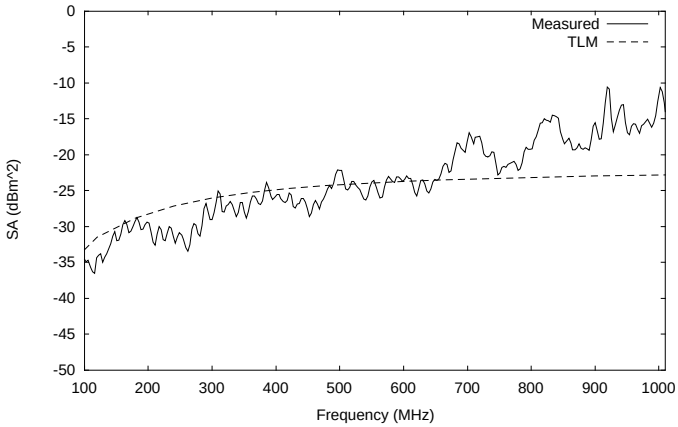

Fig. 8. The effective Shielding Aperture of the Representative Contents with no enclosure present.

The agreement between the simulation and the measurement is reasonable over most of the frequency range from 100 MHz to 800 MHz beyond which the measured absorbed power is greater than the TLM estimate based on computing the absorbed power using the Poynting vector formulation. It is believed that the estimate of R_{sm} may be the cause of the discrepancies at the higher frequencies. Below 100 MHz there was a lack of sensitivity in the development experimental system. The SA of a number of enclosures with apertures has been measured using the RC of Fig. 1. The SA of a 300 mm by 300 mm by 120 mm conducting enclosure with an aperture of 135 mm by 15 mm representing a CD drive aperture (see Fig. 9) is shown in Fig. 10a and the SA of the same enclosure with a 90mm by 10mm slot representing a floppy disk aperture is shown in Fig. 10b. Fig. 9 shows the layout of the type of enclosure used here with the position of its slot in the front face. Each aperture is in the centre of one of the 120 mm by 300 mm faces, its longest edge being

parallel to the longest dimension of the face. The RC inside the enclosure is at the enclosure's geometric centre. The incident wave direction is normal to the face with the slot and polarized such that its electric field is parallel to the shorter dimension of the slot and the face.

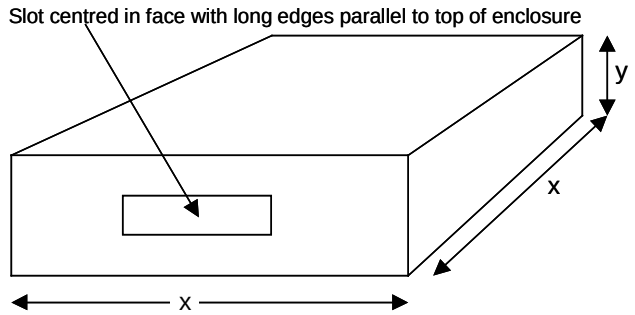

Fig. 9. Showing layout of enclosures with position of aperture (x and y are either 300 mm and 120 mm or 480 mm and 125 mm respectively depending on the enclosure used)

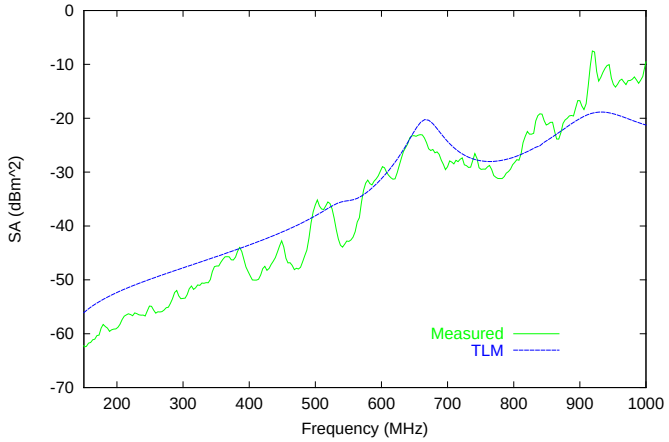

Fig. 10a. Measured and computed SA of a 300 mm by 300 mm by 120 mm enclosure with a CD sized aperture.

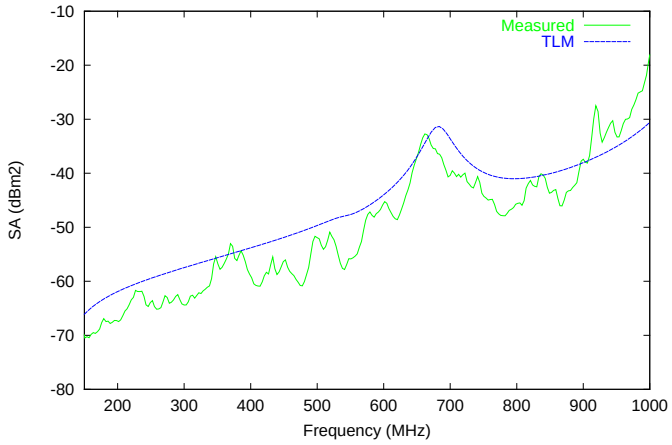

Fig. 10b. Measured and computed SA of a 300 mm by 300 mm by 120 mm enclosure with a floppy disk sized aperture.

In each case the computed SA (TLM) is based on the Poynting vector formulation. Again agreement between the computed values and the measured values is good in Figs. 10a and 10b. In all cases the measurements follow the damped resonant trend of the TLM simulations.

The shielding effect of the enclosure containing the RC can be assessed by examining the difference between the power absorbed by the RC in free space and that absorbed by the RC in the enclosure, the difference between the data of Fig. 8 and those of Fig. 10 a and b. This is shown for the computed SA values in Figs. 11a and 11b corresponding to Figs. 10a and 10b. For comparison, computations of the conventional SE values of the enclosure are also shown in Figs. 11a and 11b. The SE values were calculated at the center of the enclosure.

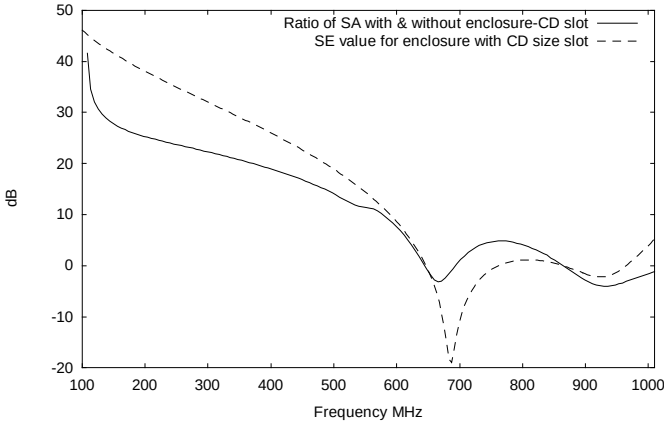

Fig. 11a. Comparison of the computed reduction in absorbed power with the SE data for the 300 mm by 300 mm by120 mm enclosure with the CD sized aperture.

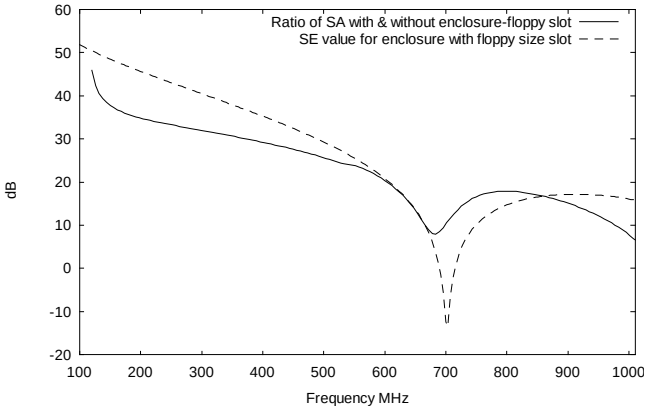

Fig. 11b. Comparison of the computed reduction in absorbed power with the SE data for the 300 mm by 300 mm by120 mm enclosure with the floppy disk sized aperture.

Note that the SE values are plotted such that negative values correspond to increased internal fields to allow direct comparison with the SA ratios. In each case it can be seen that the conventional SE over estimates the effect of the enclosure over most of the frequency range, the reduction in absorbed power being less than the SE value indicates.

The SE values are computed for an empty enclosure and the high Q values result in field enhancement at the enclosure resonance. In contrast, the damped resonant behavior of the SA values lead to much lower Q values. The SE value is related to the electric field at the geometric centre of the

enclosure whilst the SA value is the aggregate of the power absorbed over the entire surface of the RC and represents power flow over a significant fraction of the internal volume of the enclosure.

The absorbed power when the RC is in the enclosure is also enhanced in some cases at the higher frequencies but over a wider frequency range than the internal field enhancement the SE values indicate. The degree of enhancement is also less.

The 200 mm square RC represents a reasonable fill of the 300 mm square enclosure. In the case of the 480 mm by 480 mm by 125 mm enclosure with a CD sized aperture in the centre of one of the 480 mm by 125 mm faces a larger RC is appropriate. Fig. 12 represents a 400 mm square RC made from the same material as the 200 mm square RC of Fig. 1. This RC utilizes the 200 mm square RC with its sensing loops as one quarter of the 400 mm square RC. In Fig. 12 the five positions of the sensing loop pairs are indicated as 'real' sensors. The 'virtual' sensor positions are realized by moving the real sensors to the positions of the virtual sensors. In this way the RC can allow the measurement of up to twenty paired sets of surface magnetic field. Measurements of SA were made with five, nine and twenty sample sets as indicated by the ellipses in Fig. 12.

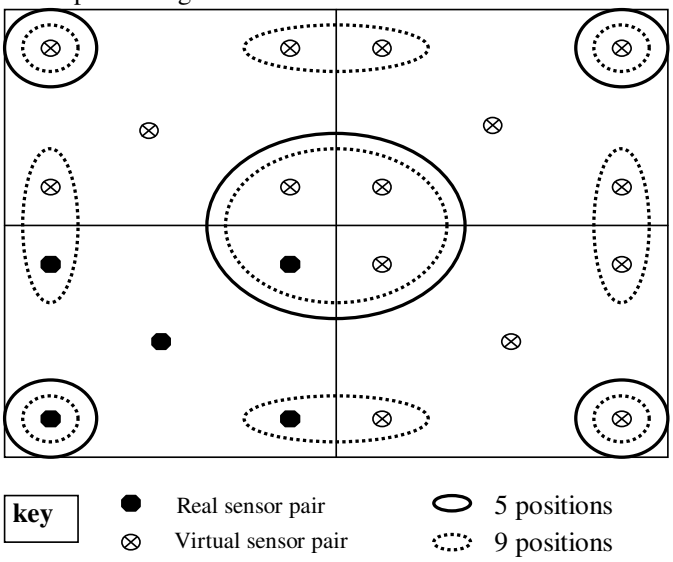

Fig. 12. Representation of the 400mm square RC showing 'real' and 'virtual' sensor pair positions.

Where more than one sensor pair is shown in an ellipse, the average field values for all sensor pairs within the ellipse are taken to assign a pair of values for center of that ellipse position. For twenty sample pairs, all the sensor positions are used. The results of these SA measurements are shown in Fig. 13 along with the TLM prediction based on evaluating the power flow (Poynting vector) over a surface surrounding the RC. The agreement is such that a five-sensor pair measurement scheme is also adequate to evaluate the SA for this RC – enclosure combination although the estimate is lower than the estimates for nine and twenty points, particularly at higher frequencies where the half wavelength loop spacing criterion is exceeded. Note that the frequency range of Fig. 13 starts at 200 MHz as the noise floor on the measured SA values is around –70 dBm^2 in the system used for these measurements.

Fig. 14 shows the difference in SA made by the larger enclosure compared to the conventional SE values. The frequency dependence is significantly different for SA and SE in this case, thus emphasizing the effect of the contents on the system performance. The SE over estimates the enclosure's effect over most of the frequency range.

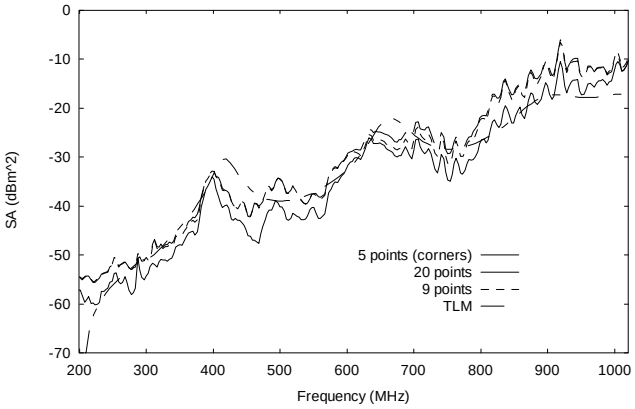

Fig. 13. Measured and computed SA for a 480 mm by 480 mm by 125 mm enclosure with a CD sized aperture and 400 mm square load for five, nine and twenty measurement points.

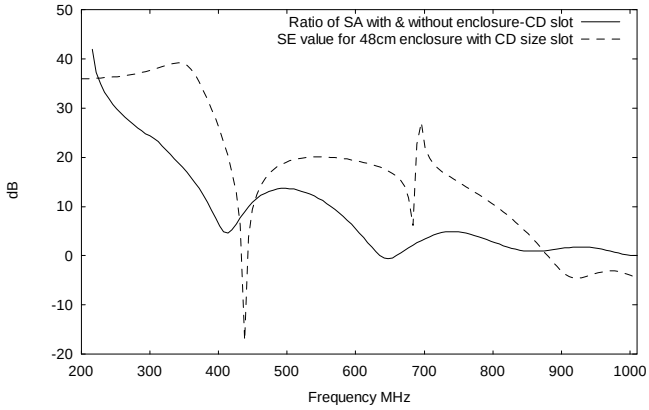

Fig. 14. Comparison of the computed reduction in absorbed power with the SE data for the 480 mm by 480 mm by125 mm enclosure with the CD sized aperture.

VI. Conclusion

In this paper a new method of assessing the efficacy of a shielding enclosure has been described. The method is applicable to enclosures used to shield electronic equipment from external interference where apertures are present to enable ventilation or disk insertion. The measure, termed here Shielding Aperture, enables an estimate of the power absorbed by the representative contents of the enclosure to be

made for a given external power density or field strength incident upon the enclosure. The representative contents can be tailored to replicate electronic systems used in the enclosures of differing sizes and device technologies. The measurement is made in a conventional EMC test chamber as used for immunity measurements. The measurement technique described here uses a network analyser as both the power source and the receiver. It can be adapted to use the signal generator and measurement receiver combination found in most test facilities if required.

The results presented here demonstrate the practicality of the technique applied to small enclosures up to 19 inch rack size (480 mm). There is no fundamental limit on the size of enclosure to which the technique could be applied. It has been shown that the conventional measure, the Shielding Effectiveness can over estimate the efficacy of the enclosure at all but resonant frequencies and that the power flow into the enclosure contents has a frequency response different to that of the SE.

The technique is formulated around the immunity of equipment and does not address the emissions from equipment in an enclosure directly. The technique is based on the scalar addition of power over the surface of the representative contents. Reciprocity cannot be directly applied. In the emissions case an enclosed electronic system radiating power from a number of points on its surface at a single frequency requires phasor addition of all contributions to estimate the total radiated fields. If the emissions are uncorrelated broadband noise within the observation bandwidth then the scalar addition used in the immunity technique is applicable. The result of the phasor addition of the contributions is determined by the relative phase of each and may exceed that resulting from the scalar sum. In these cases the over estimate of the effect of the enclosure provided by the SE will be even more apparent.

If adopted the technique requires refinement. Standardisation of the RC structures is required and the relationship between the absorbed power and the onset of interference needs to be established. The current manual switching of the connections to the field sensing loops requires automation. The technique is more time consuming than simple SE measurement techniques, however the potential benefits may outweigh this.

REFERENCES

[1] MIL-STD 285, "Method of Attenuation Measurement for Enclosures, Electromagnetic Shielding, for Electronic Test Purposes," U.S. Government Printing Office, Washington, DC, 1956.

[2] IEEE-STD 299, "Standard Method for Measuring the Effectiveness of Electromagnetic Shielding Enclosures," Institute of Electrical and Electronics Engineers, Piscataway, NJ, 1991.

[3] A Ogunsola, 'Harmonization of Shielding-Effectiveness Standards for Enclosures' Compliance Engineering (online), available at http://www.ce-mag.com/archive/01/Spring/Ogunsola

[4] F Ustuner, A Akses, I Araz, B Colak 'A method for Evaluating the shielding Effectiveness of Small Enclosures' 2001 IEEE EMC International Symposium, Washington

[5] L O Hoeft, B Bergsrund, T Young, 'Measured Electromagnetic Shielding of Small Composite Enclosures/Junction Boxes' 2001 IEEE EMC International Symposium, Washington 2001

[6] T Clupper, 'A new PCB-level shielding technology', Interference Technology, 2003, pp187-195

[7] [7]M P Robinson, S J Porter & P Op gen Oorth, "Reflection and Transmission coefficients of printed circuit boards" EMC Europe 2000, Brugge, September 2000.

Andrew C. Marvin (M'85) received the M.Eng and Ph.D degrees from the University of Sheffield, Sheffield, U.K., in 1974 and 1979, respectively.
He is Professor of Applied Electromagnetics at the University of York, York, U.K. and Technical Director of York EMC Services Ltd. His research interests include electromagnetic compatibility (EMC) measurement techniques, EMC shielding measurements, EMC antenna design, and equipment design techniques for EMC.
Dr. Marvin is currently chairman of the Management Committee of COST 286 (EMC in diffused Communications Systems), delegate to URSI panel A, and an Associate Editor of the IEEE Transactions on EMC. He is a chartered Engineer in the U.K. and a member of the Institution of Electrical Engineers, U.K.

John F Dawson (M'90) is a senior lecturer and member of the Applied Electromagnetics Research Group at the University of York, England. He received his BSc and DPhil degrees from the University of York in 1982 and 1989. His research interests include numerical electromagnetic modeling, electromagnetic compatibility prediction for circuits and systems, electromagnetic compatibility test environments, and optimisation techniques for EMC design.

Linda Dawson is a Research Fellow in the Applied Electromagnetics Research Group at the University of York, England. She gained her B.Sc. and D.Phil. degrees from the University of York in 1983 and 1990. After spending 8 years carrying out commercial consultancy and testing work she returned to the research field where her interests are mostly in the area of measurement techniques for EMC.

Janet Clegg is a research fellow with the Applied Electromagnetics Group at the Department of Electronics, University of York, UK. She received her BSc and DPhil degrees from the University of York, Department of Mathematics in 1988 and 1992. Her research interests include computational electromagnetics; application of evolutionary computation optimisation methods; electromagnetic measurement environments, screened rooms and mode stirred chambers; optimisation methods for traffic modelling.

Simon Ward was a Research Fellow in the Applied Electromagnetics Research Group at the University of York, England from 1999 to 2002. He now works for Accent Optical Technologies, York.

Axel Weissenfeld is a student at the University of Hannover, Germany. He spent 6 months on an exchange visit with the applied electromagnetic research group at the University of York, England.